# Cronfa - Swansea University Open Access Repository

_____

This is an author produced version of a paper published in:
_Marine Geology_

_____

Cronfa URL for this paper:

http://cronfa.swan.ac.uk/Record/cronfa50806

_____

**Paper:**

_____

http://www.swansea.ac.uk/library/researchsupport/ris-support/

# Computational modelling of morphodynamic response of a macro-tidal beach to future climate variabilities

William G. Bennett[a], Harshinie Karunarathna[a,*], Dominic E. Reeve[a], Nobuhito Mori[b]

[a] College of Engineering, Bay Campus, Swansea University, SA1 8EN, UK
[b] Disaster Prevention Research Institute, Kyoto University, Kyoto, Japan

A B S T R A C T

Global climate variabilities have the potential to impact many coastlines around the world, and can have detrimental effects on the stability of coastlines and their function as natural coastal defenses. This paper investigates the impacts of future extreme storms and sea level rise on morphodynamics of the macro-tidal Sefton Coast, UK, taking a process-based model as a tool to simulate a snap-shot of future beach change during storms. Sefton Coast represents one of the largest dune systems in the UK, where frontal dunes function as a natural barrier against extreme conditions. Future storm conditions were determined from global predictions of future waves at the end of the twenty first century. Future sea levels were determined based on climate change allowances set by the UK Environment Agency (EA), while future surge conditions were determined based on the guidelines also provided by EA.

A nested numerical modelling approach, that combined a regional scale model with a local scale model with high resolution, is used. The modelling suite was first validated against measured waves, water levels and beach change, before using it to simulate morphodynamic change from numerous statistically significant 'future' storm conditions. Future storm-induced morphodynamic change of the Sefton coast was then compared with that from the present storms. The results reveal that this beach will experience significant climate change driven impacts where dune retreat during storms will be considerably higher in future. The results also reveal that due to the shape of the beach and its orientation to predominant wave approach direction, there will be a strong longshore variability of morphodynamic response to storms. It was also found that the water level in front of the dune (and hence surge and future sea level rise) is the most critical factor that determines beach erosion during a storm.

## 1. Introduction

There is increasing concern among coastal planners and coastal communities about the likely effects of climate change on beach stability and coastal flooding. Recent extreme events such as the winter storms of 2013/14 in the UK have raised the profile of how susceptible coastal systems can be to coastal flooding and erosion. Winter storms can cause significant, non-recoverable impacts, and any changes to their characteristics in future will in turn affect coastal morphology, flood frequency and coastal safety. Considering Sea-Level Rise (SLR) alone, increasing average water levels in the longer-term will mean that current extreme (e.g. 1 in 100-year return period) water levels will occur with greater frequency in the future (Harley and Ciavola, 2013).

Climate change impacts on coastal environmental variables (waves, surges, wind, tides) are highly regional (Church et al., 2013; Mori et al., 2013; Hemer et al., 2013; Yasuda et al., 2014; Mori et al., 2016). For example, future projection of sea level rise shows regional differences in the spatial range of O(500 km) and strongly depends on the ocean circulation system (Church et al., 2013). The projection of wave climate shows regional differences in the range of O(100 km) (e.g. Hemer et al., 2013). The current expected future changes in global mean wave heights and wave directions ranges in ± 10% and ± 30 deg., respectively. Such wave climate changes, together with sea level rise, are expected to have significant impacts on beach morphology. Spatial variability of surges can be of very fine scale. There are significant uncertainties involved when projecting future changes to those variables at regional scales. Spatial patterns of changes in wave climate for example show large fluctuations, (Semedo et al., 2013; Shimura et al., 2015). The geomorphology of coastlines is also critical in beach response to future variabilities of these hydrodynamic forcing.

Current coastal management procedures in the UK and elsewhere rely heavily on historic measurements and extrapolating past trends and behaviours into the future. The success of this approach depends on the length, availability and the quality of historic datasets and also the assumption that past trends will continue into the future. Further, although long term trends of changes are important, extreme episodic events tend to impose greater, sometimes catastrophic, damages on coastlines and coastal defences. For example, the great flood of 1953 forced 24,000 people out of their homes and led to the deaths of over 300 people, alongside significant financial costs (Lowe et al., 2001). This highlights the need to utilise the latest techniques and research to investigate the impacts of future extreme conditions accurately in order to determine the necessary level of coastal protection for the future. With recent developments in sophisticated coastal morphodynamic modelling techniques (Lesser et al., 2004; Roelvink et al., 2009), it is now possible to model morphodynamic changes of a wide range of coastal systems. Combination of the latest projections of future sea levels and waves (Shimura et al., 2015; Environment Agency, 2017) with state of the art morphological modelling techniques allows detailed investigations of the impacts of global climate change variabilities on beach morphodynamics and flooding.

Numerous previous studies on climate change impacts on beach change have been reported. Ranasinghe (2016) gives a comprehensive review of previous literature on coastal change in a changing climate. However, most published literature have focus micro- or meso-tidal beach systems and a significant knowledge gap in the understanding of morphodynamic behaviour of macro-tidal beaches to future change in extreme conditions still exists. The objective of the present study is to investigate the impacts of global climate variabilities on coastal morphodynamics of macro-tidal beaches, focusing on episodic extreme conditions. Here we have taken the Sefton Coast located in the Liverpool Bay of the United Kingdom as a case study. Sefton has very distinct morphodynamic characteristics as a result of its macro-tidal regime and frontal dune systems. A process-based numerical modelling approach is used. 'Current' and 'future' extreme conditions were determined from global climate/wave models. Using a nested modelling approach combining the state-of-the-art Delft3D (Lesser et al., 2004; Booij et al., 1999) and XBeach (Roelvink et al., 2009) models, current and future morphodynamic change of this beach from a range of statistically significant 'current' and 'future' extreme conditions are modelled.

This paper is structured as follows: Sections 2 and 3 describe the case study area, and the methodology to derive storm conditions and the modelling approach respectively. The results and discussion are given in Sections 4 and 5, with conclusions drawn in Section 6.

## 2. Study site

The Sefton Coast is located in Liverpool Bay in the northwest of England (UK), between the Mersey and Ribble estuaries (Fig. 1). The 36 km coastline is transitional between open coast and estuarine regimes, influenced by processes both in the eastern Irish Sea and in the adjacent estuaries (Pye, 1990). The coastline contains a diverse range of environments additional to the estuaries, with tidal flats, salt marshes, defended sections, recreational beaches, and substantial frontal dunes. The dune system of the Sefton coast is the largest in England and Wales. Dunes extend from Liverpool to Southport, with a maximum width of 4 km at Formby Point (Pye and Blott, 2008).

The Sefton coast is macrotidal with a mean spring tidal range exceeding 8 m (Saye et al., 2005; van der Wal et al., 2002), specifically 8.22 m at Liverpool and 9.56 m at Heysham (Esteves et al., 2011). Significant wave height in Liverpool Bay during storms is found to be around 5.5 m (Brown et al., 2011). The mean annual significant wave height is 0.53 m (Esteves et al., 2011). Positive surges of around 0.5 m frequently occur at Liverpool Bay but an extreme storm surge of 2.4 m has been recorded (Brown et al., 2010). Waves within Liverpool Bay show little variation in approach direction, with the majority of waves

reaching from 240°-300° (Wolf et al., 2011).

Soaking of the dune toe and subsequent wave undercutting, which leads to slumping of the dune face has been found to be the main driver behind Sefton dune retreat (Pye and Blott, 2008). Dune erosion of the Sefton coast is reported when extreme storm surge and wave events coincide with spring-high tides, where water levels reach the dune toe. (Pye and Blott, 2008; Halcrow, 2010). Some sections of the Sefton coast are vulnerable even during smaller storms, whilst the most severe storm events cause erosion of the entire dune frontage (> 1 in 10-year events) (Pye and Blott, 2008).

In a study of global climate change-induced changes to future wave conditions in Liverpool Bay, it was found that extreme storm conditions may become more frequent and intense in future, however more typical storms conditions may become less frequent (Brown et al., 2011). As a result, coastal erosion will be less frequent but it will be more extreme when it does occur. In the meantime, future mean sea level will be higher thus contributing to increased dune erosion and flooding in future (Blott et al., 2006; Esteves et al., 2011).

## 3. Methodology

### 3.1. Determination of storm boundary conditions for the model

To computationally model the morphodynamics of Sefton Coast, storm boundary conditions should be determined. This includes future storm wave, wind and water level (tides and surge) conditions. Storm conditions were chosen encompassing frequent events (1 in 1, 1 in 5 year return levels), through to extreme events (1 in 100 year return level) that are considered for coastal defence design purposes, providing an understanding of the coastlines response to a range of storm events.

### 3.1.1. Storm surge

Dynamic projection of future storm surge at regional scale is difficult due to its spatial variabilities and low occurrence probability. Therefore, we use a simplified statistical approach to implement future changes in storm surge considering climate change here.

Statistically significant water level boundary conditions during storms for the model are obtained based on McMillan et al. (2011). Using data supplied by the National Tide and Sea Level Facility of the UK (NTSLF), they performed a statistical analysis to determine peak water levels and storm water level profiles using the Skew Surge Joint Probability Method (SSJPM) for 40 of the UK national network (class A) tide gauge sites from around the coastlines of England, Scotland and Wales, together with equivalent data from 5 other primary sites. The skew surge is defined as the excess water level above the predicted tidal high-water level during a storm (de Vries et al., 1995). Probabilities of predicted high tide and of skew surge have been combined to give overall design sea level probabilities, expressed in terms of levels attributed to their respective average return period. To provide continuous coverage for the entire coastline an interpolation method has been used to determine sea levels with a range of return periods, assisted with the use of a continental shelf tide-surge model. A series of corrections has been applied to obtain the design sea values. Model results for extreme sea level values at the primary gauge sites have first been corrected to correspond with the statistical analysis data. The model provided return period extreme sea levels at intermediate points at 12 km spacing between the primary gauge sites. At the intermediate points model results have been adjusted according to a proportional difference in model variations and the observed data at the primary sites. This allowed for the variation of physical processes along the coast. Linear interpolation between model nodes has been used to provide results at 2 km spacing. A final check and adjustment have been done to ensure return period levels were plausible. This was achieved through comparing design sea level values with the high water levels between 1 in 1 and 1 in 200 year return periods provided by the
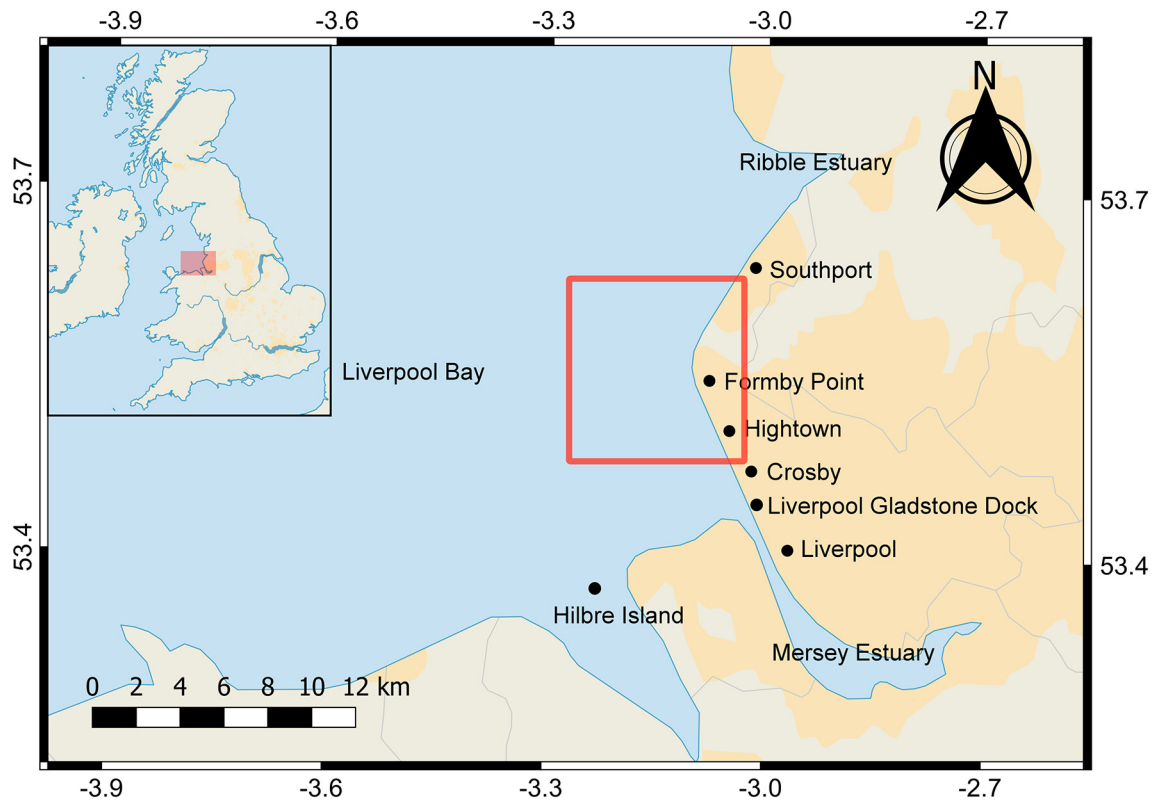
**Fig. 1.** A map of Liverpool Bay and Sefton Coast, UK. The red box highlights the section of coastline studied. (For interpretation of the references to colour in this figure legend, the reader is referred to the web version of this article.)

secondary tide gauge data.

During extreme tide levels, the total tidal curve is a combination of the astronomical tide, and the storm surge. Design surge profiles, such as the one for Liverpool Gladstone Dock (ref. Fig. 1 for location) shown in Fig. 2, have been used to derive appropriate total water level curves, by providing a representation of the surge shape, defining the increase and decline over time. These skew surge-based design surge profiles have been determined by first extracting the 15 largest surge events recorded at each of the 40 Class A Tide Gauge sites in the UK over a period of 18 years between 1991 and 2009. To create design surge profiles, several methods have been assessed to provide a precautionary but not conservative assessment of flood risk. From this, the time-integrated surge method is adopted to generate the surge profiles. In this method, first the time varying surge was plotted for each of the 15

events. Outlier events that were not representative of the predominant surge shape were ignored; further details are provided in McMillan et al. (2011). Then, they were standardised to provide normalised surge profiles. With a peak value of 1, for comparison. The duration of each of the 15 surges at particular levels of normalised surge magnitude (i.e. 10%, 20% etc.) have been calculated. The maximum duration at each level has then been calculated and arranged to form the surge shape by determining the relative proportions of the duration expected on the rising and falling limbs of the surge. The surge shape was then smoothed. Further details of the method can be found in McMillan et al. (2011).

To provide the base astronomical tidal boundary conditions, the MATLAB tidal fitting toolbox T_TIDE was used (Pawlowicz et al., 2002). 35 tidal constituents were calculated by applying Fast Fourier
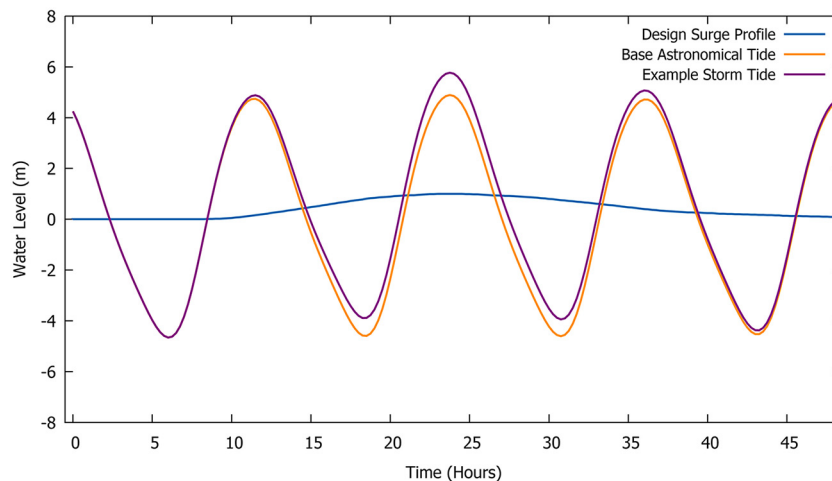


**Fig. 2.** An example design surge profile (McMillan et al., 2011), base astronomical tide and the storm tide.

**Table 1**
SSJPM results for Liverpool, Gladstone Dock.

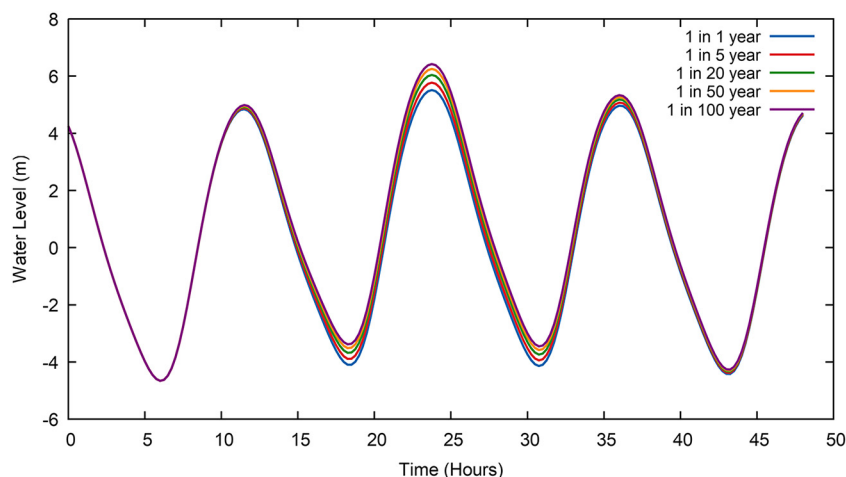| Return Period (years) | 1 | 2 | 5 | 10 | 20 | 25 | 50 | 75 | 100 | 150 | 200 |
|---|---|---|---|---|---|---|---|---|---|---|---|
| Peak Sea Level (mOD) | 5.51 | 5.62 | 5.77 | 5.90 | 6.04 | 6.09 | 6.25 | 6.35 | 6.42 | 6.52 | 6.60 |



**Fig. 3.** Design storm water level profiles generated through the approach of McMillan et al. (2011) for 1 in 1, 5, 20, 50, and 100-year return period storm events.

Transformation (FFT) to decompose the observed water level record at Liverpool Gladstone Dock tide gauge. These 35 constituents were then utilised to predict the desired tidal elevation. Following the method suggested by McMillan et al. (2011), the base astronomical curve was generated through prediction of a peak water level halfway between Mean High Water Spring tide (MHWS) and Highest Astronomical Tide (HAT), in this case 4.95 m Ordnance Datum (OD), using the tidal constituent analysis.

In order to generate the final water level profile with different return periods, the base astronomical curve was upscaled using the desired peak water level (Table 1) and the design surge profile. These events do not include a surge value such as the maximum recorded 2.4 m, as the highest surges do not coincide with high tidal levels due to the local effect of tide surge interaction (Brown et al., 2010). The results are summarised in Fig. 3. In this case it is considered that the storm peaks at high tide to represent the worst case extreme event scenario.

To provide future storm water levels, McMillan et al. (2011) recommends superposition of the relevant SLR projection on to the present water level profiles. The Environment Agency (EA) of UK provides climate change allowances based on predictions of anticipated change for a range of variables (EA, 2017). These allowances are not based on a single scenario. They are informed by the latest climate change projections from different global models, and scenarios of emissions to the atmosphere and, provide different values for different epochs over the next century. EA allowances for sea level rise provided in Table 2 were used for this study.

*3.1.2. Storm waves*

To generate storm wave conditions in both present and future climates, the global wave projections of Shimura et al. (2015) are used. The dynamic wave projections have been carried out using the WAVEWATCH III v3.14 wave model (Tolman, 2009) forced Sea Surface Temperature (SST) using high-resolution Atmospheric Global Climate Model (AGCM) projections under the Inter-governmental Panel for Climate Change (IPCC) A1B scenario. The 60 km resolution AGCM used was the MRI-AGCM3.2H (Mizuta et al., 2012), developed by the Japanese Meteorological Research Institute, and used for IPCC AR5 (IPCC, 2013). The model has been forced by four typical Sea Surface Temperature (SST) conditions from the Coupled Model Inter-comparison

Project 3 (CMIP3) (Covey et al., 2003). The global domain for wave projections was set for the latitudinal range of 90° S-−67° N over all longitudes with 60 km spatial grids. Wave projections have been done for two time slices: 'Current' wave projections correspond to the time period of 1979–2009 and future projections corresponding to the time period of 2075–2100.

Projected wave outputs from the model nodes were extracted and filtered for storm conditions using the storm event definition of Dissanayake et al. (2015) and using a storm wave height threshold of 2.5 m, based on the UK Channel Coastal Observatory (CCO) guidance (www.channelcoast.org/reports/). The details of storm definition and the method used to isolate storm events are given in Bennett et al. (2016). Projected storm data were then bias corrected using measured storms extracted from the West Hebrides and Pembroke WaveNet buoys (Fig. 4) (Bennett et al., 2016). The bias correction applied to the projected data was the mean ratio. This techniques adjusts the uncorrected data through use of the ratio between the means of the measured and projected datasets. The corrected projected conditions are calculated by multiplying by this ratio, such that the mean of the corrected projected data is equal to the mean of the measured data. The bias corrected projected storm conditions were then used to generate statistically significant storm wave conditions as follows:

First, the peak significant wave height of each isolated storm identified according to the storm definition described above were then identified. Then, the Generalised Pareto Distribution (GPD) was fitted to the peak storm wave heights. The GPD is given in Eq. (1) (which is the combination of three statistical families), and the method of Hawkes et al. (2002) was used. In Eq. (1), $\phi$ and $\xi$ are scale and shape parameters respectively (Coles, 2001) and $u$ is the threshold that ensures model convergence. The R statistical software package *ismev* (Coles, 2001) was utilised to fit GPD to data (R Core Team, 2013).

$$Pr\{X > x \mid X > u\} = \begin{cases} 1 + \xi\,\phi^{-1}\,(x - u)^{-1/\xi} & \xi \neq 0 \\ e^{-\frac{x-u}{\phi}} & \xi = 0 \end{cases} \tag{1}$$

The significant wave height under 'present' climate, $H_{s,\,p}$ for storm conditions corresponding to 1 in 1, 5, 20, 50, and 100-year return periods were derived from the GPD, the return level plots are shown in Fig. 5. This range of return periods was chosen as they represent a

**Table 2**
Environment Agency sea level rise (SLR) value guidelines (Environment Agency, 2017).

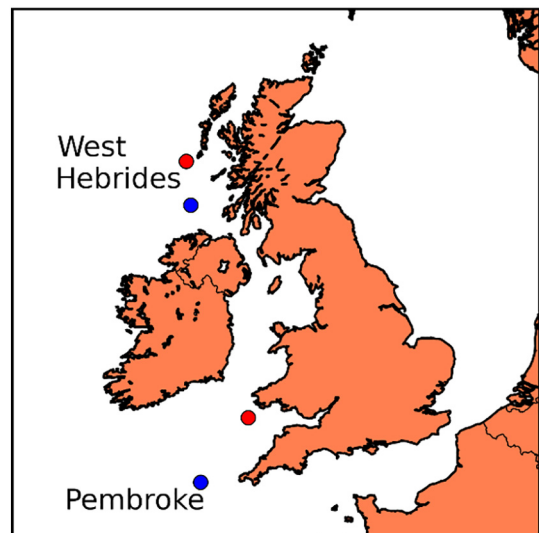| Area of England | 1990–2025 mm/yr (mm) | 2026–2055 mm/yr (mm) | 2056–2085 mm/yr (mm) | 2086–2115 mm/yr (mm) | Cumulative SLR 1990–2115 (m) |
|---|---|---|---|---|---|
| East, east midlands, London, south east | 4 (140) | 8.5 (255) | 12 (360) | 15 (450) | 1.21 |
| South West | 3.5 (122.5) | 8 (240) | 11.5 (345) | 14.5 (435) | 1.14 |
| North west, north east | 2.5 (87.5) | 7 (210) | 10 (300) | 13 (390) | 0.99 |



**Fig. 4.** Wave boundary locations (blue dots. (Shimura et al., 2015)), with observed wave records used for bias correction (red dots). (For interpretation of the references to colour in this figure legend, the reader is referred to the web version of this article.)

variety of storm events which will induce impacts between medium and high-risk, and useful for coastal and flood defence design. The maximum storm wave period ($T_{max}$) was determined from the average of the $T_{max}$ values for individual storms extracted from the projected data. Due to the small variation in wave approach direction during storms events, the predominant direction across all the individual storm events was used as the incident storm direction ($Wd_{avg}$). These conditions are summarised in Table 3.

Similar analysis was carried out for 'future' storms, in order to generate statistically significant future storm conditions. In this case, wave projections derived under the ensemble mean of the IPCC (2007) A1B scenario were used. The $H_{s, p}$ values under future storm conditions corresponding with 1 in 1, 5, 20, 50, and 100-year return periods are given in Table 4. Similar to the 'current' condition, the storm wave period was determined from the average of the modelled storm data. Predominant wave direction during storms was used as the storm direction.

To provide wind forcing required for the computational model, wind outputs from the corresponding Global Climate Model (GCM) simulations (Shimura et al., 2015) were extracted for Liverpool Bay (Fig. 4), and filtered for wind velocities ($U_{10}$) during storm conditions. As with the wave data, the GPD was fitted to the wind data. The predominant wind direction was determined from observed wind data collected at Hilbre weather station (Fig. 1) due to the coarse resolution of the model outputs and the complex regional behaviour. The storm duration was also investigated via the same approach. The return level plot for the 'present' storm wind velocity is shown in Fig. 6, and the wind and duration conditions are summarised in Table 5.

To provide time series wave and wind boundary conditions for the model during storms with different return periods, representative measured storm profiles were developed using peak storm wave and wind conditions developed above (Fig. 6). It was found that a three-point spline curve provided a good representation of a storm profile when compared with observed storms (Fig. 7). In the storm profile developed using the three-point spline curve, start and end points of the storm profile have the threshold wave height used for isolation of storms from the wave data, and the mid-point the peak storm wave height generated using GPD occurring halfway through the storm duration. The corresponding wind conditions for the chosen storm wave return period follow the same three-point spline shape.
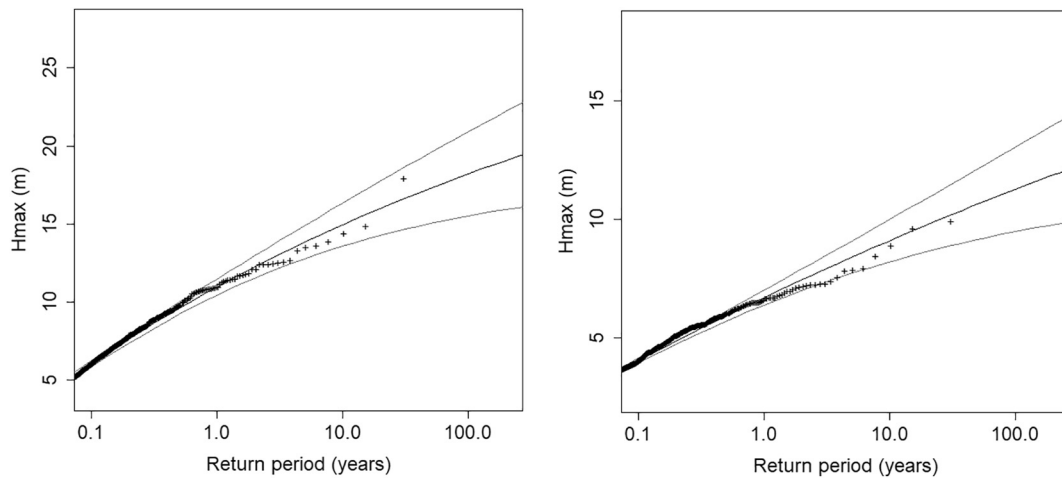
**Fig. 5.** GPD profiles for present climate north (left) and south (right) storm boundary points. Crosses indicate storm significant wave height values, with the GPD fit and 95% confidence intervals indicated by the three curves.

**Table 3**
Summary of 'present' statistically significant storm boundary conditions at Pembroke and West Hebrides. $H_{s,p,n}$ ($n$ = 1, 5, 20, 50, 100) refers to 'present' peak significant storm wave height with return period $n$. $T_{max}$ is the maximum storm wave period, and $Wd_{avg}$ is the predominant storm wave direction.

| Location | $H_{s, p, 1}$ | $H_{s, p, 5}$ | $H_{s, p, 20}$ | $H_{s, p, 50}$ | $H_{s, p, 100}$ | $T_{max}$ | $Wd_{avg}$ |
|---|---|---|---|---|---|---|---|
| Pembroke | 6.70 | 8.40 | 9.77 | 10.63 | 11.26 | 7.35 | 200 |
| West Hebrides | 10.95 | 13.83 | 16.00 | 17.29 | 18.21 | 10.26 | 285 |

**Table 4**
Summary of future storm wave boundary conditions at Pembroke and West Hebrides.

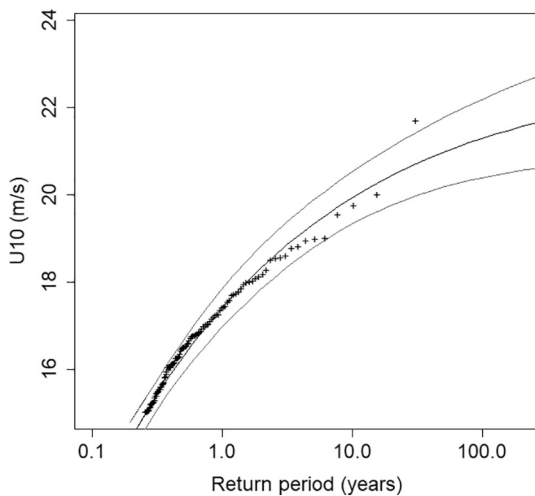| Location | $H_{s, p, 1}$ | $H_{s, p, 5}$ | $H_{s, p, 20}$ | $H_{s, p, 50}$ | $H_{s, p, 100}$ | $T_{max}$ | $Wd_{avg}$ |
|---|---|---|---|---|---|---|---|
| Pembroke | 6.74 | 8.34 | 9.55 | 10.28 | 10.8 | 7.14 | 200 |
| West Hebrides | 11.12 | 13.39 | 14.85 | 15.62 | 16.12 | 9.86 | 285 |



**Fig. 6.** GPD profile for 'present climate' $U_{10}$ at at Liverpool Bay. Crosses indicate observed storm values, with the GPD fit and 95% confidence intervals indicated by the three curves.

### 3.1.3. Selection of storm events

To encompass a range of potential storm impacts on the Sefton coast, storm scenarios were derived by combining statistically significant peak storm wave height, surge, and storm duration. A total of

**Table 5**
Wind boundary forcing (U10 velocity and predominant direction) derived using GPD fitted to modelled wind data at Liverpool Bay determined from GCM (Shimura et al., 2015), for both 'present' and 'future' climate conditions.

| Return Period (years) | 1 | 5 | 20 | 50 | 100 | Predominant direction |
|---|---|---|---|---|---|---|
| Present $U_{10}(ms^{-1})$ | 17.3 | 19.5 | 21.2 | 22.2 | 22.9 | 270 |
| Future $U_{10}(ms^{-1})$ | 17.4 | 19.3 | 20.4 | 21.0 | 21.3 | |
| Duration (hours) | 67 | 111 | 154 | 186 | 212 | |

76 'present' and 'future' storms were selected to be modelled, representing a range of present and future climate storm scenarios. Eight storms providing a cross section of the results were chosen for analysis of the spatial morphodynamic impacts. The details of the eight selected storms presented are given in Table 6, with further details of all selected storm conditions found in Bennett (2017). The selected scenarios cover more frequent storms and rarer extreme events. The wave and surge boundary conditions are combined such that the peak wave coincides with the peak water level during storms, thus representing the worst case scenario for each combination of conditions.

### 3.2. Computational Modelling approach

To investigate morphological changes induced by extreme events, it was necessary to combine several numerical models and domains. Two different models were combined and three model domains were nested in a set up to optimise computational time, and to accurately represent the Sefton Coast and dune system. Transformation of storm waves from the GCM boundary point locations described in Section 3 was carried out using the Delft3D (Lesser et al., 2004) WAVE module. This model provided wave and water level boundary forcing for a coupled Delft3D WAVE & FLOW model. Wave and water level conditions from this model were subsequently applied for the boundary of a high resolution, local scale morphological model developed using XBeach (Roelvink et al., 2009).

For the shelf-scale Delft3D WAVE model domain A (Fig. 8), a 1 km resolution cartesian grid spanning between the Pembroke and West Hebrides wave boundary points (Fig. 4), and covers the entire the Irish Sea, St. George's Channel, Bristol Channel, and extending in to the Celtic Sea, was created. The bathymetry for this domain was taken from the GEBCO08 dataset (Becker et al., 2009). The model is forced by non-stationary hourly wind and storm wave information. This large computational domain allows the propagation of both swell and wind waves into the area of interest. 48 h of model spin-up time was allowed for stability and accurate results, and to provide spin-up time for the
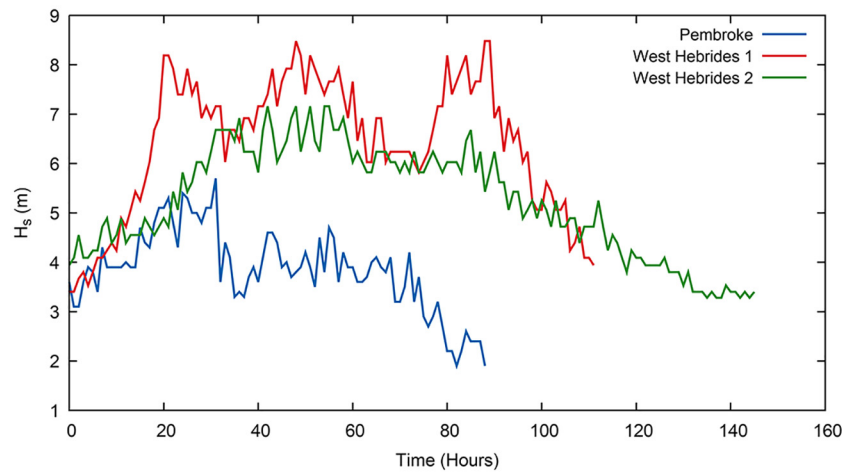
Fig. 7. Example storm profiles from observed Pembroke and West Hebrides WaveNet wave buoy data.

**Table 6**

Selected subset of storm conditions used for the analysis. Storm events are labelled with the convention, Peak storm wave height return period_Water level return period_Duration return period (Bennett, 2017).

| Present storm events | Peak storm wave height return period | Water level return period | Peak storm wave height (m) | Water level (m) | Duration (hours) |
|---|---|---|---|---|---|
| 20_20_1 | 20 | 20 | 4.84 | 6.04 | 67 |
| 20_100_1 | 20 | 100 | 4.84 | 6.42 | 67 |
| 100_20_1 | 100 | 20 | 5.36 | 6.04 | 67 |
| 100_50_1 | 100 | 100 | 5.36 | 6.25 | 67 |
| 1_1_5 | 1 | 1 | 3.62 | 5.51 | 111 |
| Future Storm Events | | | | | |
| 20_20_1 | 20 | 20 | 4.60 | 6.78 | 67 |
| 100_50_1 | 100 | 100 | 4.86 | 6.99 | 67 |
| 1_1_5 | 1 | 1 | 3.65 | 6.25 | 111 |

nested models. Wave data (significant wave height, wave period, wave direction) for the whole area were stored at hourly time intervals to provide boundary forcing for the nested smaller model domains.

The wave model was validated against storm wave data measured by Liverpool Bay WaveNet Wave buoy (CEFAS). Modelled 1 in 1, 5, 20, 50, and 100-year return period peak storm wave heights under 'present' climate showed reasonable agreement with those determined from observed storm wave data, with an average under-prediction of 14% (Fig. 9). The under-prediction of peak storm wave height by the model may be due to the resolution of the GCM model runs, which may not have predicted the local wind well enough to accurately capture the wind sea.

The nested model Domain B (Fig. 8) is utilised in the combined Delft3D WAVE and FLOW modules in order to provide water level and wave boundary conditions for a smaller XBeach morphodynamic model, domain C. The curvilinear grid for domain B, which covers the majority of the Sefton coastline, was created using the RGFGRID facility in Delft3D. Domain B has coarser resolution grid cells (300 m × 1000 m in cross-shore & alongshore directions) along the offshore boundary,
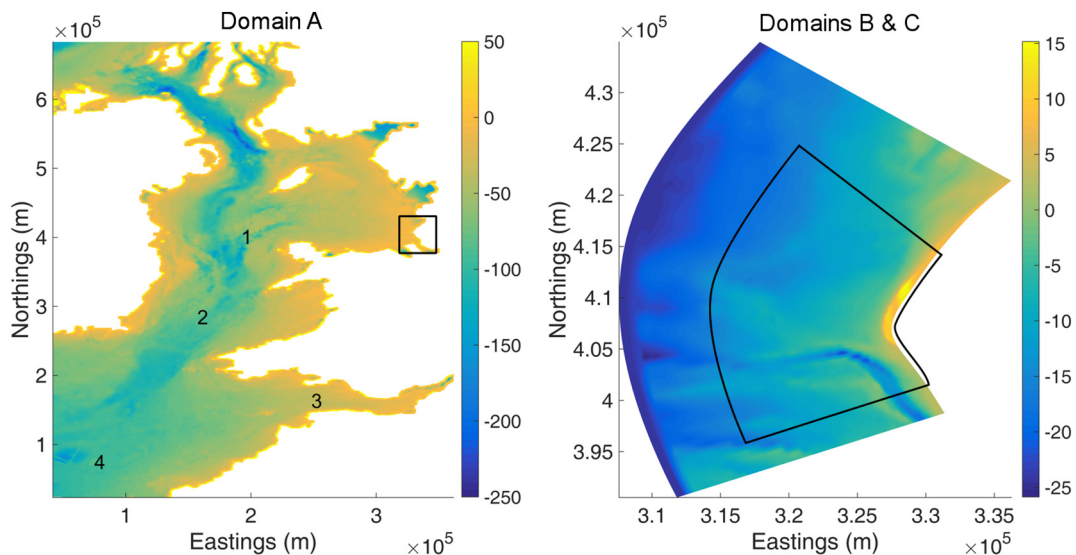


Fig. 8. Model domains. Domain A (left) covers the area between the two storm boundary points used in this study. Model bathymetry for domain A was generated from the GEBCO08 dataset (Becker et al., 2009). Numbers 1, 2, 3, and 4 highlight the Irish Sea, St George's Channel, Bristol Channel and Celtic Sea respectively, with the Sefton coastline location highlighted in black. Model domain B (right) of the coupled Delft3D WAVE and FLOW domain covering the Sefton coastline and extending out in to Liverpool Bay. Model bathymetry for domain B, generated using POLCOMS bathymetry data (Brown et al., 2010). Domain C of the XBeach domain, highlighted in black (right), extends from Sefton dune crest to -18 m ODN offshore and covers the longshore distance from Crosby to Southport. (For interpretation of the references to colour in this figure legend, the reader is referred to the web version of this article.)
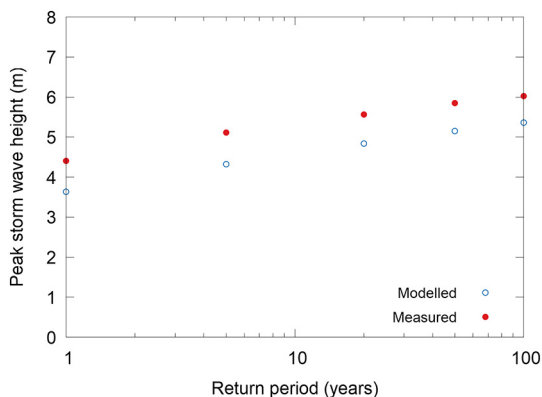
**Fig. 9.** 1 in 1, 5, 20, 50, and 100-year return level peak storm wave heights determined from modelled and measured waves.

and higher resolutions cells closer to the shoreline (25 m × 600 m). The bathymetry of this model is established using 90 m resolution POLCOMS model bathymetry (Brown et al., 2010). The POLCOMS model bathymetry extends from +5 m ODN to -50 m ODN (Williams et al., 2011). To cover the bathymetry of the Sefton dune system, LiDAR data set from airborne laser scan transects carried out on the 14th March 2010, with 1 m × 1 m resolution was used (Gold, 2010). The offshore boundary was set at -25 m ODN, and the offshore grid cells were set at a constant depth to ensure offshore uniformity of boundary forcing.

Wind and wave boundary forcing for the domain B are taken from domain A. The water level boundary condition at the southern offshore point of the model domain B is created using McMillan et al. (2011), as aforementioned in Section 3.1.1. The northern water level point is determined by applying the phase shift between the south and north lateral tidal boundaries (Dissanayake et al., 2014). To calculate this phase difference, tidal elevations from the POLCOMS model (Bricheno et al., 2013) corresponding to the north and south boundary points of domain B were used. Each tidal signal was decomposed into 35 tidal constituents using Fast Fourier Transform (FFT). Then, a comparison of the predicted tidal elevations at both the north and south points provides the forward phase shift of 8 min 38 s between the north and south

boundary points. Both Delft3D WAVE and FLOW models were online coupled, to include wave-current interaction, with communication between flow and waves at 30 min intervals. Water level and wave outputs at the offshore boundary of domain C (Fig. 8) were saved at 15 min intervals.

Domain C uses XBeach coastal area model (Roelvink et al., 2009) to determine morphodynamic change and wave overtopping at Sefton Coast. Whilst it is acknowledged that subtidal dynamics are not well captured by XBeach model, the focus of this study is on dune erosion, for which XBeach is intended and has been extensively tested and validated worldwide. The high resolution domain C covers the highly dynamic beach and dune system surrounding Formby Point of the Sefton Coast. The alongshore length of domain C at the land boundary is approximately 15 km. The offshore grid cells of domain C are of lower resolution (140 m × 70 m in cross-shore x alongshore directions) with the grid refining towards onshore to 2 m × 25 m closer to the shoreline. The bathymetry datasets utilised are the same as those used for the domain B. For all three domains, the grid size and resolution were chosen to achieve accurate results while optimising computational time. Simulations were run on the state-of-the-art Supercomputing Wales high performance computing cluster (https://www.supercomputing.wales), providing extensive computational power.

XBeach has previously been extensively calibrated for Liverpool Bay by Dissanayake et al. (2014). In their study, a storm event that occurred in March 2010 was used to validate the Liverpool Bay XBeach morphodynamics model. Modelled beach profile change during March 2010 storm at five cross shore locations (Williams et al., 2011) were compared with modelled cross-shore profile change. The model performance was rated using Root Mean Square Error (RMSE), Residual Sum of Squares (RSS), and Brier Skill Score (BSS) (van Rijn and Walstra, 2003). Dissanayake et al. (2014) found that mean RMSE, RSS and BSS for their validation were 0.31, 0.82, and 0.89 respectively, which confirms that the model is able to capture morphodynamic change during the storm event satisfactorily. While the calibration of XBeach may vary under different storm conditions, considering the macrotidal nature of the coastline, and the availability of data, these model parameters were used for the storm simulations.
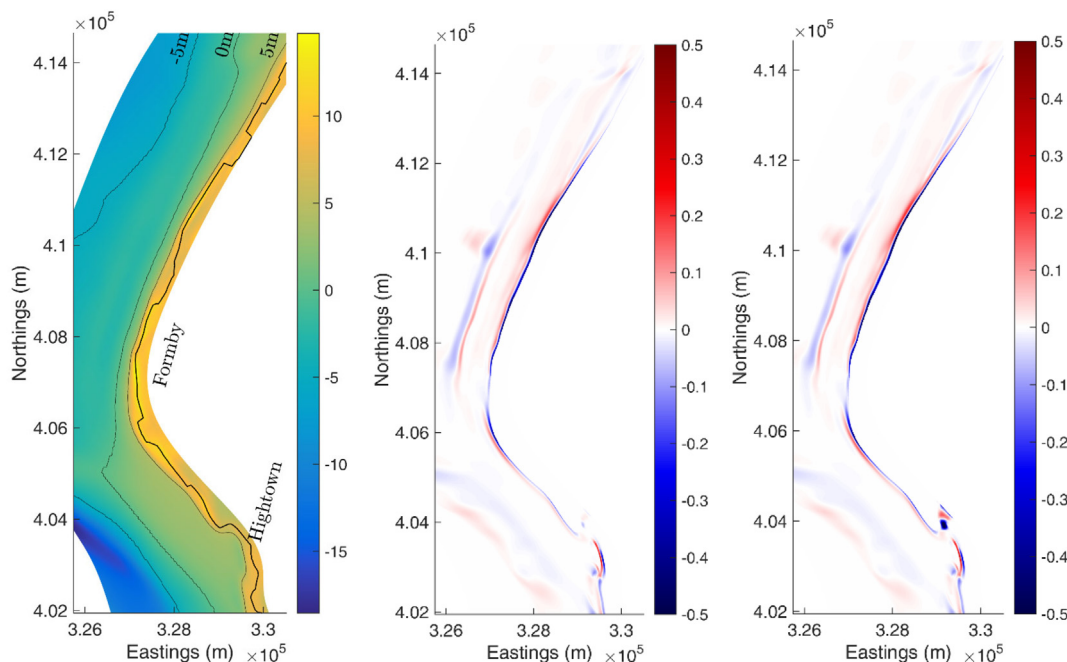


**Fig. 10.** Comparison of present sea bed change at Sefton Coast as a result of 20_20_1 (centre), 20_100_1 (right) storms (colour bar in metres). Initial bathymetry with contours and dune crest (thick black line) (left) displayed as a reference.
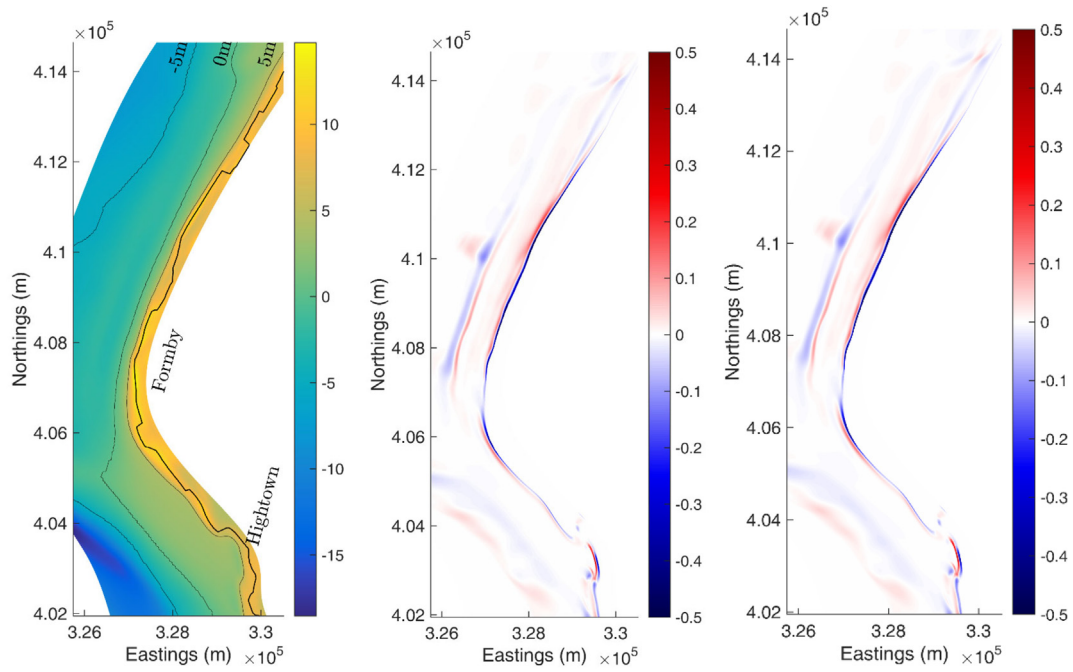
**Fig. 11.** Comparison of present sea bed change at Sefton Coast as a result of 20_20_1 (centre), 100_20_1 (right) storms (colour bar in metres). Initial bathymetry with contours and dune crest (thick black line) (left) displayed as a reference.

## 4. Results

This section presents and discusses the morphodynamic change of Sefton Coast during present and future storm events, based on the morphodynamics simulations carried out using the storms and modelling approach described in Section 3.

### 4.1. Effect of peak storm wave height and water level

Figs. 10, and 11 show morphodynamic change along the Sefton Coast from a variety of storm wave conditions under the 'present'

climate conditions described in Table 6. Figs. 12, 13, and 14, however, focus on the impacts of climate change under the future storms provided in Table 6. Focusing on the intertidal area and dune system, which is the most active part of the beach, the initial bed level, with the -5 m, 0 m, and 5 m depth contour lines and the dune crest, are shown alongside the changes in these figures as a reference. The patterns of erosion and accretion provide insights into the links between the hydrodynamic forcing during storms, and their impacts on beach morphodynamics.

In Fig. 10, the bed level changes from the 20_20_1 and 20_100_1 storm events are displayed alongside their differences, highlighting the
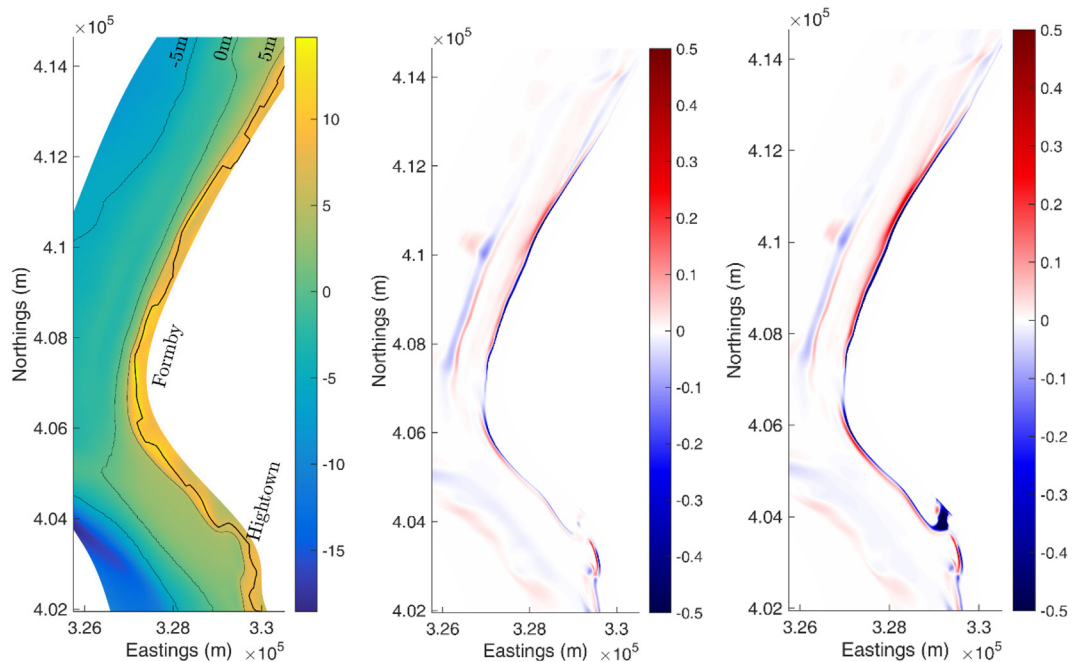


**Fig. 12.** Comparison of the sea bed change from the 'present' 20_20_1(centre) and 'future' 20_20_1 (right) storms (colour bar in metres). Initial bathymetry with contours and dune crest (thick black line) (left) displayed as a reference.

**Fig. 13.** Comparison of sea bed change from the 'present' 100_50_1(centre) and 'future' 100_50_1 (right) storms (colour bar in metres). Initial bathymetry with contours and dune crest (thick black line) (left) displayed as a reference.
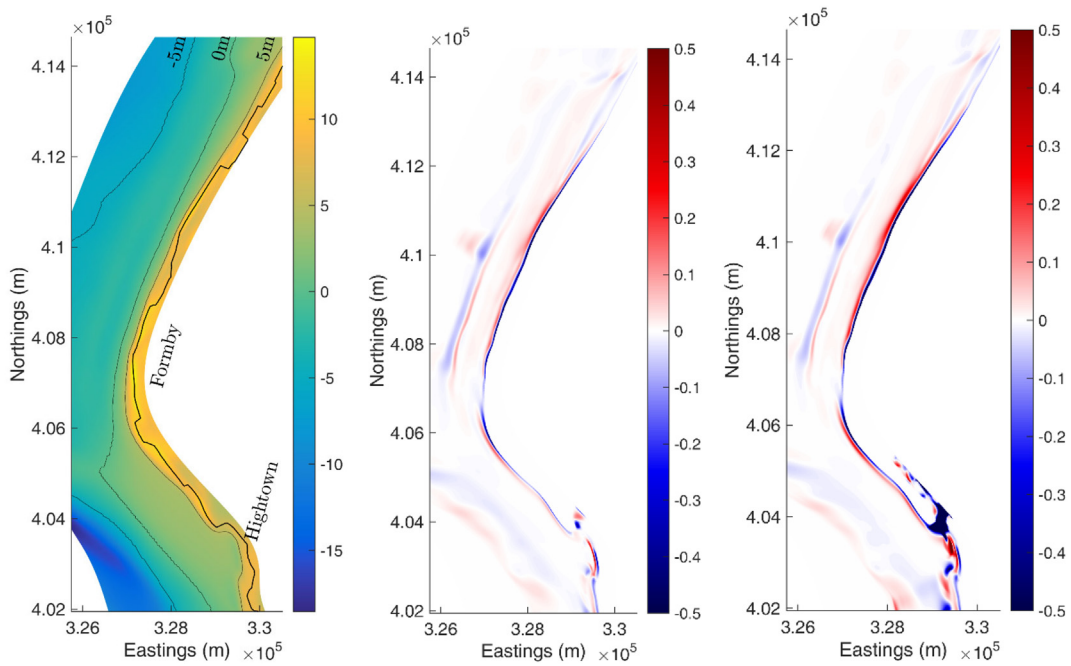


**Fig. 14.** Comparison sea bed change from the 'present' 1_1_5 (centre) and 'future' 1_1_5 (right) storms (colour bar in metres). Initial bathymetry with contours and dune crest (thick black line) (left) displayed as a reference.
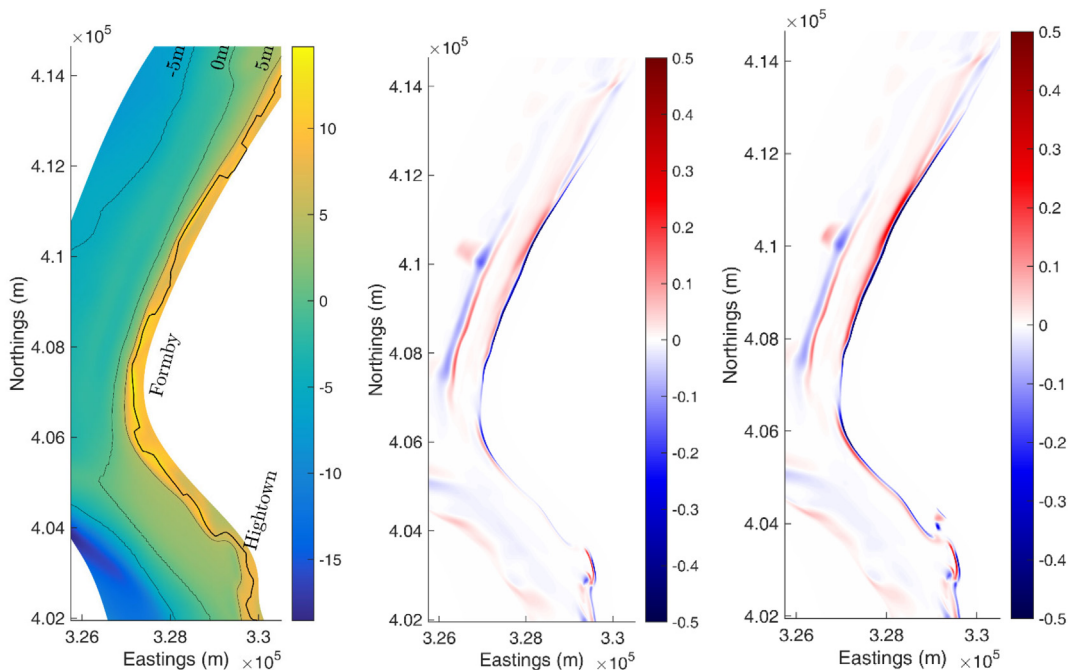
impact of the water level on the morphological impacts. A slight flattening of an offshore bar feature is observed, as well as patterns of small scale erosion and accretion between the 0 m and -5 m contours. For both storm events the areas with significant erosion are located along the less sheltered section north of Formby Point. Most changes are observed near the 5 m depth contour (around the dune foot). Small-scale erosion can be seen at the 1 km stretch of the coastline south of Formby Point. There is a pattern of flattening of the beach face closer to the south lateral boundary of domain C near Hightown, which becomes more severe with the increase in water level, although not as large as the erosion to the north of Formby Point. The most significant

difference between the morphology change during the two storm events is noted across the dune crest near Hightown. It can be seen that 20_100_1 storm overwashes the dune crest significantly, while there is an increase in erosion near the 5 m contour with the more severe water level, the accretion lower down the beach profile spreads over a larger area.

In Fig. 11 the impacts of changing extreme storm wave height are investigated, by contrasting the morphodynamic change during the present 1 in 20 and 1 in 100-year storm wave conditions. The water level during both storms has a 1 in 20-year return period. Even though there is 0.52 m difference of peak storm wave height between the

storms, only slight differences are observed in terms of morphological change. The majority of differences are at the 5 m depth contour around Formby Point, while some differences are seen near Hightown. Overall, morphological changes during these two storms are very similar, indicating the fact that morphodynamics of this beach is more sensitive to the water level during a storm than the peak storm wave height.

### 4.2. Impacts of climate change on morphodynamics

For investigating the impact of climate change, firstly, the morphodynamic change of Sefton coast during the 'present' and 'future' 20_20_1 storm events are compared (Fig. 12). There is a clear difference in the pattern of erosion in the areas north of Formby Point and south of Hightown, with increased severity of the impacts on the dune face under future storm conditions. The alongshore extent of dune inundation at Hightown during the future 20_20_1 storm will be larger than that from the present storm with same return period.

The stretch of the coast around and north of Formby Point exposed to south-westerly storms, and the areas south of Hightown show significant beach lowering (> 0.3 m) in the supratidal zone. Similar to Fig. 10, Fig. 12 also shows accretion in the lower intertidal zone, corresponding with the increase in erosion on the dune face. Therefore, the increase in water level due to sea level rise in future leads to substantial increase in morphological activity, with much more of the coastline being affected than under present climate conditions.

Fig. 13 highlights the dramatic increase in morphological change during the future extreme 100_50_1 storm, when compared to that from the current storm with same return period. Large scale impacts are evident across the whole coastline during the future 100_50_1 storm event, as a result of the extreme water level of 6.99 m ODN. The addition of sea level rise on the 1 in 50-year extreme water level, leads to a large amount of overwashing and inundation near Hightown, and dune erosion at and north of Formby Point. Alongside this, there is significant sediment deposition in the lower intertidal areas.

In Fig. 14, present and future sea bed change from a longer duration but less severe storm (1_1_5) are investigated. Although the storm wave conditions are of a much lower magnitude, the longer duration of the storm seems to induce significant morphodynamic changes along the coastline north of Formby Point. The magnitude and pattern of the changes occurred under the present 1_1_5 storm is similar to those occurred during the 20_20_1 (present) storm shown in Fig. 14. As the future 1 in 1-year peak storm water level exceeds the present 1 in 20-year water level, overwashing of the dune system near Hightown is also seen during the future 1_1_5 storm. While under the present climate, erosion of the dune toe is limited to the section north of and including Formby point, in future this extends along a greater stretch of the coastline. The future 1_1_5 storm displays erosion towards the northern extent of the domain, and along the stretch further south between Formby and Hightown.

Figs. 15 and 16 summarises the dune volume loss from the complete set of storm conditions used in this study under 'present' and 'future' climate conditions. The loss in dune volume is defined as the total volume of sediment removed from the dune face between the 5 m contour and the dune crest per metre of coastline. In these two figures, the loss in dune volume is plotted against the storm power index for each storm. The storm power index gives the severity of a storm based on storm wave heights and storm duration, and calculated following the procedure of Dissanayake et al. (2015). Under the 'present climate' storms (Fig. 15), the dune volume loss shows a strong positive correlation with increasing storm power. However, the difference due to the peak storm water level is more apparent, with large differences between the 1 in 1, 5 and 20-year values. During the 'future climate' storms (Fig. 16), the positive trend with storm power is less evident, where the water level primarily defines the loss in dune volume. Compared to the present climate, the 1 in 1 and 1 in 5-year return period future peak storm water level conditions show similar magnitudes of dune volume
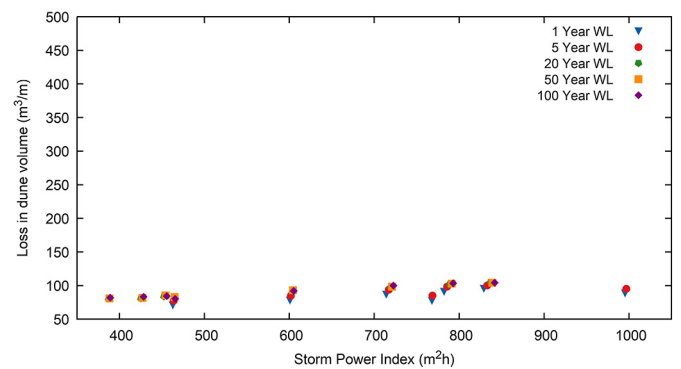


**Fig. 15.** The loss in dune volume plotted against the storm power index for the full set of 'present climate' storm simulations.
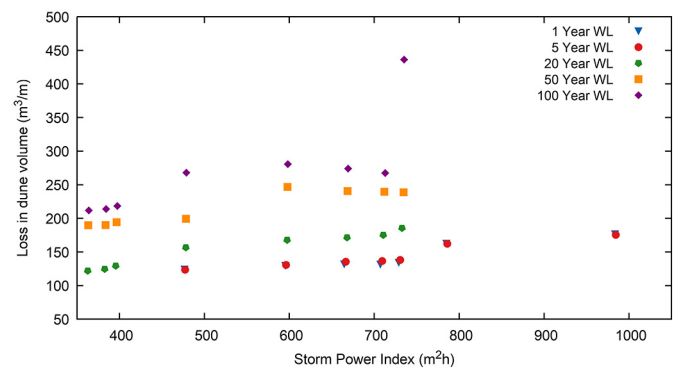


**Fig. 16.** The loss in dune volume plotted against the storm power index for the full set of 'future' climate storm simulations.

losses. With the impact of sea level rise the 1 in 20, 50 and 100-year return level conditions show large differences, highlighting the importance of the peak storm water level.

### 4.3. Cross-shore profile change

To investigate the morphodynamic response to extreme storms at specific locations along the Sefton coastline which are found to be highly dynamic and of interest to coastal managers, pre- and post-storm cross-shore profiles from the modelled data are analysed in detail. For this study, cross-shore profiles 10, 12, 15, 18, and 19 (Fig. 17), which represent key cross-sections of the Sefton Coast considered for coastal management purposes by the Sefton Council where significant dune erosion takes place, are selected. Figs. 18–22 display profile changes at the selected profiles during the storm events given in Table 6.

Profile 10 (P10) is located to the south of Formby Point, at the vulnerable dune section identified in Figs. 10, 12 and 13. It is characterised by a lower dune crest than the majority of the Sefton Coast. P10 shows significant overwashing and erosion of the dune under the selected future storm conditions (Fig. 18), as the peak storm water level nears and exceeds the level of the dune crest. Under the present climate conditions, erosion of the dune crest is minor, with only small impacts from overtopping. However, in future, the whole dune crest will be lowered by approximately 0.75 m and 1.75 m as a result of 20_20_1 and 100_50_1 storm events respectively. This highlights the vulnerability of this section of the Sefton Coast to future climate change, especially SLR.

P12, located to the south of Formby Point (Fig. 17), is characterised by a steep dune face and gentle inter-tidal beach slope, is exposed to south-westerly storms. P12 shows erosion and scarping of the dune under the selected storm conditions (Fig. 19). The dune face above 5 m ODN of P12 undergoes erosion, with varying severity under different storm conditions. It is clear that 'future' storm conditions will induce
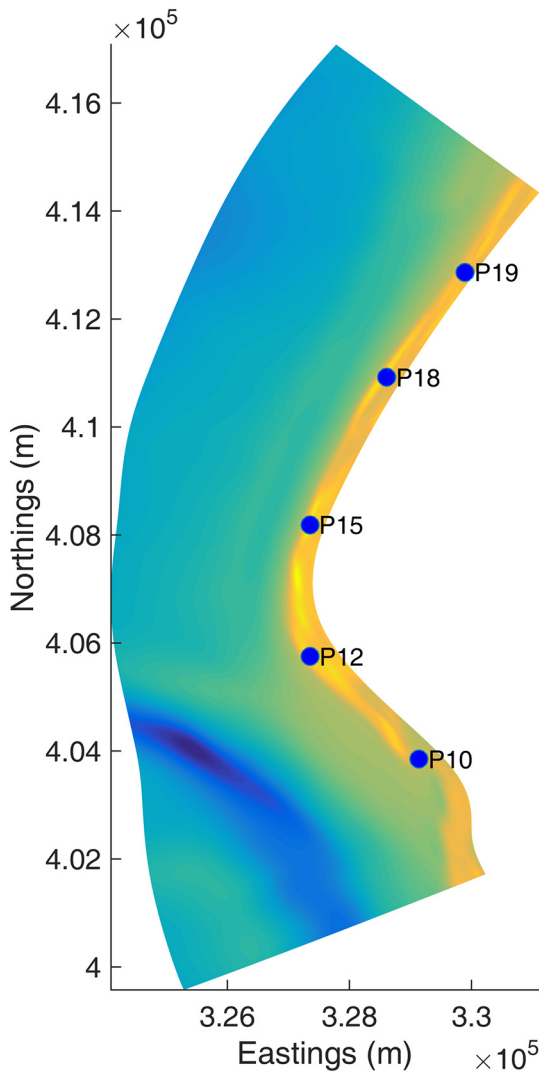
**Fig. 17.** Locations of the highly dynamic historical cross-shore transects used to investigate detailed morphodynamic change.
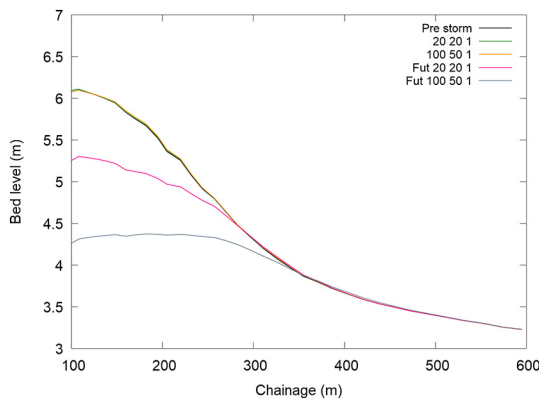


**Fig. 18.** Comparison of post-storm cross shore profiles from a selection of 'present' and 'future' storms at P10.



**Fig. 19.** Comparison of post-storm cross shore profiles from a selection of 'present' and 'future' storms at P12.



**Fig. 20.** Comparison of post-storm cross shore profiles from a selection of 'present' and 'future' storms at P15.



**Fig. 21.** Comparison of post-storm cross shore profiles of a selection of 'present' and 'future' storms at P18.

significantly severe dune erosion at this location. The largest dune retreat occurs from the future 100_50_1 storm, where approximately 25 m retreat was found. For this event, the eroded sediment from the dune system is redistributed in the intertidal area between ~200 m and ~270 m offshore, flattening and raising the beach profile. Under present storm conditions the maximum retreat is ~12 m, highlighting the
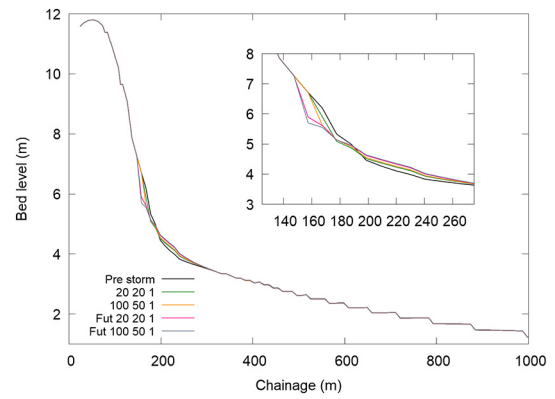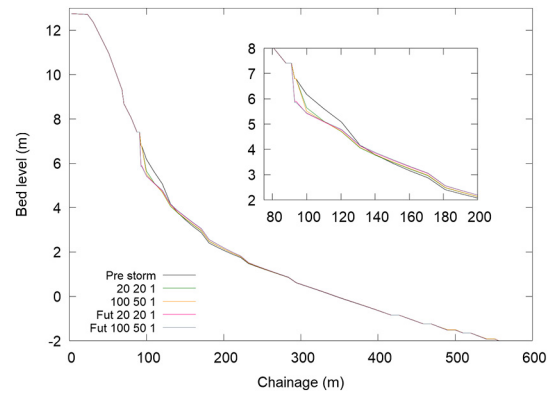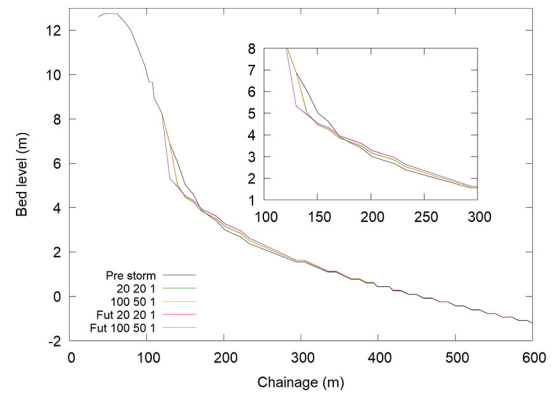
severity of future impacts. It is clear that the extent of the storm impact at P12 depends on the severity of the storm condition, with a substantial difference in erosion of the dune face as a result of the present and future climate storms.

Profile 15, located north of Formby Point, is also characterised by a steep dune face (Fig. 20) and is exposed to south-westerly storms. This location has been identified as one of the most dynamic and vulnerable areas of the Sefton Coast (Pye and Blott, 2008; Esteves et al., 2009; Dissanayake et al., 2014). The beach profile change from all selected storm conditions show erosion above 4 m ODN with erosion of the dune taking place at different elevations corresponding with the storm severity, extending up to 7 m ODN. The future 100_50_1 storm induces the largest beach erosion with a retreat of ~20 m, while under current
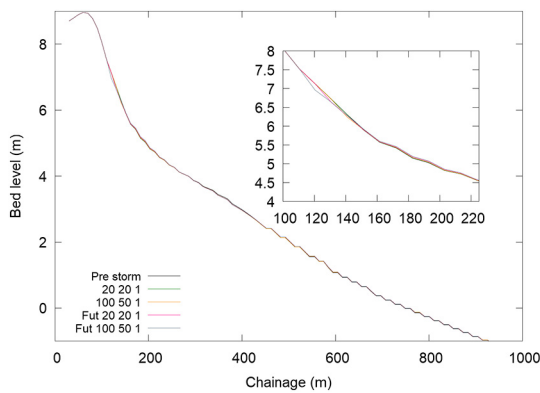
**Fig. 22.** Comparison of post-storm cross shore profiles of a selection of 'present' and 'future' storms at P19.

storm conditions the maximum retreat is ~15 m. For storms with large return period water levels, erosion of the dune face extends from ~90 m to ~130 m in the cross-shore direction. The excessive steepening of dune front may have significant implications on the stability of the dune at this location in future.

Located on the exposed stretch of coastline north of Formby point, P18 also has a steep dune face and a gentle lower intertidal slope (Fig. 21). Dune erosion at this location is similar to that of P12 and P15 where the largest profile change occurs above 4.0 m ODN. Future storms induce dune erosion significantly larger than of current storms, where the erosion during 100_50_1 extends up to 8 m ODN. The eroded sediment is redistributed in the inter-tidal zone between ~130 m and ~200 m offshore. At P18 the maximum retreat is ~25 m for the future 100_50_1 storm, while under present storm conditions the maximum retreat is ~15 m. As with P15, the steepening of the dune front is exacerbated in future and may have significant impacts on its stability.

P19, located closer to the northern end of the morphological domain C near Southport (Fig. 17), shows no significant morphological response to the selected storms (Fig. 22). The dune face at this location is less steep compared to the other profiles. With a gentle lower foreshore extending into the subtidal region, and with its partially sheltered location to the south westerly storms, P19 is less susceptible to storm erosion. The only noticeable change occurred as a result of the future 100_50_1 storm, but the maximum beach lowering is < 0.3 m, and within a small region of the supratidal zone, which is much smaller than those observed at P10, P12, P15, and P18.

## 5. Discussion

The results shown in Section 4 indicate a significant longshore variability of morphodynamic response of the Sefton Coast to storm conditions. This is mainly due to the shape of the coastline and its orientation with respect to storm approach (Pye and Blott, 2008). Historically, Esteves et al. (2012) found that the largest dune retreat occurred during the storm of 11–12 November 1977, with up to 20 m dune retreat, and flooding of properties and damage to coastal defences. They also found that dune erosion of between 5 and 14 m occurred more frequently along the Sefton Coast, while the 2013/14 winter storms induced a maximum retreat of 12.1 m near P15 (Pye and Blott, 2016). The largest storm during the 13/14 storm season occurred on the 5th–6th December, with 1 in 5-year return period wave conditions, and 1 in 44-year water level conditions (Wadey et al., 2015). This corresponds well with the dune erosion observed at these profiles, where the computational model predicted maximum dune retreat from current storms at P15 as 15 m. Compared to the maximum dune retreat of 15 m from present storms, the model predicts maximum dune retreat of 25 m during future extreme storms. Therefore, the results clearly indicate that the changes to future storm climate as a result of global

climate variabilities may have noticeably severe implications on the stability of Sefton dunes. Formby Point and the areas just north of Formby Point will remain extremely vulnerable to predominantly south-westerly storms.

The importance of water levels compared compared to storm wave height for the Sefton dune erosion is clear from the results. As a macrotidal environment, understanding the physical processes is key to the understanding of the impacts on dune erosion. Along the coastline the dune foot is located just above the mean spring high water level, and as such the peak storm water level is a key factor in determining what part of the beach face suffers most from storm wave attack. This has previously been noted along the Sefton Coastline with the identification of a critical water level for dune erosion (Pye and Blott, 2008). A water level of 5.5mOD was identified as the critical value for severe dune erosion, with 4.4mOD for dune toe undercutting. When these water levels occur, waves reach further up the beach face, with sand dragged down the slope due to erosion of the dune. This undercutting of the dune may then cause the dune face to become unstable and collapse with the sediment more prone to further redistribution by waves. Thus, the water level is more important than the wave height for defining the level of erosion for the Sefton Coastline.

This study focuses on the impacts on the dune system and upper beach of the Sefton Coastline. The limitations of XBeach in predicting subtidal dynamics highlighted in Section 3 may restrict the application of this modelling framework to cases where this is important. For example where subtidal bars are key in defining the location of wave breaking. Dynamic surge modelling to investigate the differences between present and future climate surge conditions is recommended for future studies to investigate the role of climate change on surge within the UK context in greater detail.

## 6. Conclusions

Statistically significant storm waves determined from projected waves under present and future climate conditions are used to examine morphodynamic response of the Sefton Coast to future extreme storm conditions driven by global climate change, using Delft3D-XBeach coastal models. The model correctly reproduced dune retreat during historic storm events in areas around and north of Formby Point, giving us confidence to use it for investigation of morphodynamic response of the beach to climate change-induced variations of future extreme conditions. The results clearly show how future variabilities of key coastal environmental forcings such as storm waves, surge and sea level, impact the morphodynamics of Sefton Coast. A significant longshore variability of morphodynamic response is seen as a result of the shape of this beach and its orientation to storm approach. Areas north of Formby Point and south of Hightown are found to be the most vulnerable areas of the beach. This will remain the same in future.

The largest morphological changes in the cross-shore direction were observed mostly in the upper beach and dune face. The severity of dune retreat at and north of Formby Point during storm events will increase significantly in future, compared to present conditions. In addition, future conditions seem to induce dune overwash in areas around Hightown thus exacerbating flooding and inundation. While the peak storm wave height can affect the level of beach-dune erosion, the water level during a storm is the key in determining morphodynamics of this macro-tidal coastline. Therefore, sea level rise as a result of global climate change will play a significant role on future stability of this coastline.

The approach detailed in this study provides an understanding of the impacts of 'morphodynamic shocks' induced by future storms on the integrity of the Sefton Coast, compared to the current situation. It does not however provide long term trends of behaviour when responding to future climate variabilities, which needs to be further investigated. The macro-tidal conditions and the complex beach-dune combined system makes water level at the dune the predominant factor for erosion. This

situation may be different at other beaches.

The methodology applied here can be applied at a diverse range of coastal sites around the UK and elsewhere to provide insights into future morphological response of beaches to episodic future extreme conditions anticipated as a result of global climate variabilities. The results can be very useful to improve current coastal management policy, adding to Shoreline Management Plans (SMP's) which will in turn inform new coastal defence solutions.

## Acknowledgements

## References

Blott, S.J., Pye, K., van der Wal, D., Neal, A., 2006. Long-term morphological change and its causes in the Mersey Estuary, NW England. Geomorphology, 81 (1–2):(185–182-206).

Becker, J.J., Sandwell, D.T., Smith, W.H.F., Braud, J., Binder, B., Depner, J., Fabre, D., Factor, J., Ingalls, S., Kim, S.-H., Ladner, R., Marks, K., Nelson, S., Pharaoh, A., Trimmer, R., Von Rosenberg, J., Wallace, G., Weatherall, P., 2009. Global bathymetry and elevation data at 30 arc seconds resolution: SRTM30_PLUS. Mar. Geod. 32 (4), 355–371.

Bennett, W.G., 2017. Climate Change Impacts on Coastal Flooding and Erosion. PhD Thesis. Swansea University, United Kingdom.

Bennett, W.G., Karunarathna, H., Mori, N., Reeve, D.E., 2016. Climate Change Impacts on Future Wave climate around the UK. Journal of Marine Science & Engineering 4, 78.

Booij, N., Ris, R.C., Holthuijsen, L.H., 1999. A third generation wave model for coastal regions, part I, model description and validation. J. Geophys. Res. 104 (C4), 7649–7666.

Bricheno, L.M., Wolf, J.M., Brown, J.M., 2013. Impacts of high resolution model downscaling in coastal regions. Cont. Shelf Res. 87, 7–16.

Brown, J.M., Souza, A.J., Wolf, J., 2010. An 11-year validation of wave-surge modelling in the Irish Sea, using a nested POLCOMS–WAM modelling system. Ocean Model 33, 118–128. https://doi.org/10.1016/j.ocemod.2009.12.006.

Brown, J.M., Wolf, J., Souza, A.J., 2011. Past to future extreme events in Liverpool Bay: model projections from 1960--2100. Clim. Chang. 111 (2), 365–391.

Church, J.A., Clark, P.U., Cazenave, A., Gregory, J.M., Jevrejeva, S., Levermann, A., Merrifield, M.A., Milne, G.A., Nerem, R.S., Nunn, P.D., Payne, A.J., Pfeffer, W.T., Stammer, D., Unnikrishnan, A.S., 2013. Sea Level Change. In: Stocker, T.F., Qin, D., Plattner, G.-K., Tignor, M., Allen, S.K., Boschung, J., Nauels, A., Xia, Y., Bex, V., Midgley, P.M. (Eds.), Climate Change 2013: The Physical Science Basis. Contribution of Working Group I to the Fifth Assessment Report of the Intergovernmental Panel on Climate Change. Cambridge University Press, Cambridge, United Kingdom and New York, NY, USA.

Coles, S., 2001. An Introduction to Statistical Modeling of Extreme Values. Springer-Verlag, London.

Covey, C., Achuta Rao, K.M., Cubasch, U., Jones, P., Lambert, S.J., Mann, M.E., Phillips, T.J., Taylor, K.E., 2003. An overview of results from the coupled model inter-comparison project. Glob. Planet. Chang. 37 (1–2), 103–133.

Dissanayake, P., Brown, J.M., Karunarathna, H., 2014. Modelling storm-induced beach/dune evolution: Sefton coast, Liverpool Bay, UK. Mar. Geol. 357, 225–242.

Dissanayake, P., Brown, J.M., Wisse, P., Karunarathna, H., 2015. Comparison of storm cluster vs isolated event impacts on beach/dune morphodynamics. Estuar. Coast. Shelf Sci. 164, 301–312.

Environment Agency, 2017. Flood Risk Assessments: Climate Change Allowances. https://www.gov.uk/guidance/flood-risk-assessments-climate-change-allowances.

Esteves, L.S., Williams, J.J., Nock, A., Lymbery, G., 2009. Quantifying shoreline changes along the Sefton Coast (UK) and the Implications for Research-Informed Coastal Management. J. Coast. Res. 2009 (56), 602–606.

Esteves, L.S., Williams, J.J., Brown, J.M., 2011. Looking for evidence of climate change impacts in the eastern Irish Sea. Natural Hazards and Earth System Science 11 (6), 1641–1656.

Esteves, L.S., Brown, J.M., Williams, J.J., Lymbery, G., 2012. Quantifying thresholds for significant dune erosion along the Sefton Coast, Northwest England. Geomorphology 143-144, 52–61.

Gold, I., 2010. Lidar quality control report project pm_0901: Survey for polygon p_6802. In: Technical Report. Environment Agency, UK.

Halcrow, 2010. North West England and North Wales shoreline Management Plan SMP2. In: Technical Report. Halcrow Group Limited.

Harley, M.D., Ciavola, P., 2013. Managing local coastal inundation risk using real-time forecasts and artificial dune placements. Coast. Eng. 77, 77–90.

Hawkes, P.J., Gouldby, B.P., Tawn, J.A., Owen, M.W., 2002. The joint probability of waves and water levels in coastal engineering design. J. Hydraul. Res. 40 (3), 241–251.

Hemer, M.A., Fan, Y., Mori, N., Semedo, A., Wang, X.L., 2013. Projected changes in wave climate from a multi-model ensemble. Nat. Clim. Chang. 6p. https://doi.org/10.1038/nclimate1791.

IPCC, 2013. Climate Change 2013: The Physical Science Basis. In: Contribution of Working Group I to the Fifth Assessment Report of the Intergovernmental Panel on Climate Change. Cambridge University Press, Cambridge, United Kingdom and New York, NY, USA.

IPCC, 2007. Climate change, 2007. The Physical Science Basis. Contribution of Working Group I to the Fourth Assessment Report of the Intergovernmental Panel on Climate Change. Agenda.

Lesser, G.R., Roelvink, J.A., van Kester, J.A.T.M., Stelling, G.S., 2004. Development and validation of a three-dimensional morphological model. Coast. Eng. 51 (8–9), 883–915.

Lowe, J.A., Gregory, J.M., Flather, R.A., 2001. Changes in the occurrence of storm surges around the United Kingdom under a future climate scenario using a dynamic storm surge model driven by the Hadley Centre climate models. Clim. Dyn. 18 (3–4), 179–188.

McMillan, A., Batstone, C., Worth, D., Tawn, J., Horsburgh, K., Lawless, D., 2011. Coastal flood boundary conditions for UK mainland and Islands. In: Technical Report. Environment Agency.

Mizuta, R., Yoshimura, H., Murakami, H., Matsueda, M., Endo, H., Ose, T., Kamiguchi, K., Hosaka, M., Sugi, M.A., Yukimoto, S., Kusunoki, S., Kitoh, A., 2012. Climate simu-lations using MRI-AGCM3.2 with 20-km grid. J. Meteorol. Soc. Jpn. 90A (0), 233–258.

Mori, N., Shimura, T., Yasuda, T., Mase, H., 2013. Multi-model climate projections of ocean surface variables under different climate scenarios, future change of waves, sea level and wind. Ocean Eng. 71, 122–129.

Mori, N., Kjerland, M., Nakajo, S., Shibutani, Y., Shimura, T., 2016. Impact assessment of climate change on coastal hazards in Japan. review paper. Hydrological Research Letters 10 (3), 101–105. https://doi.org/10.3178/hrl.10.101.

Pawlowicz, R., Beardsley, B., Lentz, S., 2002. Classical tidal harmonic analysis including error estimates in MATLAB using TDE. Comput. Geosci. 28 (8), 929–937.

Pye, K., 1990. Physical and human influences on coastal dune development between the Ribble and Mersey estuaries, Northwest England. In: Nordstrom, K.F., Psuty, N.P., Carter, R.W.G. (Eds.), Coastal Dunes: Form and Process. John Wiley & Sons Ltd, Chichester, pp. 339–359.

Pye, K., Blott, S.J., 2008. Decadal-scale variation in dune erosion and accretion rates: an investigation of the significance of changing storm tide frequency and magnitude on the Sefton coast, UK. Geomorphology 102 (3–4), 652–666.

Pye, K., Blott, S.J., 2016. Assessment of beach and dune erosion and accretion using LiDAR: impact of the stormy 2013–14 winter and longer term trends on the Sefton Coast, UK. Geomorphology 266, 146–167.

R Core Team, 2013. R: A Language and Environment for Statistical Computing. R Foundation for Statistical Computing, Vienna, Austria.

Ranasinghe, R., 2016. Assessing climate change impacts on open sandy coasts: a review. Earth-Sci. Rev. 160, 320–332.

van Rijn, L.C., Walstra, D.J.R., 2003. The predictability of cross-shore bed evolution of sandy beaches at the time scale of storms and seasons using process-based profile models. Coast. Eng. 47, 295–327.

Roelvink, D., Reniers, A., van Dongeren, A., van Thiel de Vries, J., McCall, R., Lescinski, J., 2009. Modelling storm impacts on beaches, dunes and barrier islands. Coast. Eng. 56 (11 − 12), 1133–1152.

Saye, S.E., van der Wal, D., Pye, K., Blott, S.J., 2005. Beach–dune morphological re-lationships and erosion/accretion: an investigation at five sites in England and Wales using LIDAR data. Geomorphology 72, 128–155.

Semedo, A., Weisse, R., Behrens, A., Sterl, A., Bengtsson, L., Günther, H., 2013. Projection of global wave climate change toward the end of the twenty-first century. J. Clim. 26 (21), 8269–8288.

Shimura, T., Mori, N., Mase, H., 2015. Future projection of ocean wave climate: analysis of SST impacts on wave climate changes in the Western North Pacific. J. Clim. 28 (8), 3171–3190.

Tolman, H.L., 2009. User Manual and System Documentation of WAVEWATCHIIITM Version 3.14. Technical Note.

de Vries, H., Breton, M., De Mulder, T., Krestenitis, Y., Ozer, J., Proctor, R., Ruddick, K., Salomon, J.C., Voorrips, A., 1995. A comparison of 2-D storm surge models applied to three shallow European seas. Environ. Softw. 10 (1), 23–42.

Wadey, M.P., Brown, J.M., Haigh, I.D., Dolphin, T., Wisse, P., 2015. Assessment and comparison of extreme sea levels and waves during the 2013/14 storm season in two UK coastal regions. Natural Hazards and Earth System Science 15, 2209–2225.

van der Wal, D., Pye, K., Neal, A., 2002. Long-term morphological change in the Ribble Estuary, Northwest England. Mar. Geol. 189 (3–4), 249–266.

Williams, J.J., Brown, J.M., Esteves, L.S., Souza, A., 2011. MICORE WP4 Modelling Coastal Erosion and Flooding along the Sefton Coast NW UK, Final Report. Technical Report. Morphological Impacts and Coastal Risks Induced by Extreme Storm Events.

Wolf, J., Brown, J.M., Howarth, M.J., 2011. The wave climate of Liverpool Bay—observations and modelling. Ocean Dyn. 61, 639–655. https://doi.org/10.1007/s10236-011-0376-9.

Yasuda, T., Nakajo, S., Kim, S., Mase, H., Mori, N., Horsburgh, K., 2014. Evaluation of future storm surge risk in East Asia based on state-of-the-art climate change projec-tion. Coast. Eng. 83, 65–71.